

Community Geodetic Model V1: Horizontal Velocity Grid

David Sandwell, Yuehua Zeng, Zheng-Kang Shen, Brendan Crowell, Jessica Murray, Rob McCaffrey and Xiaohua Xu

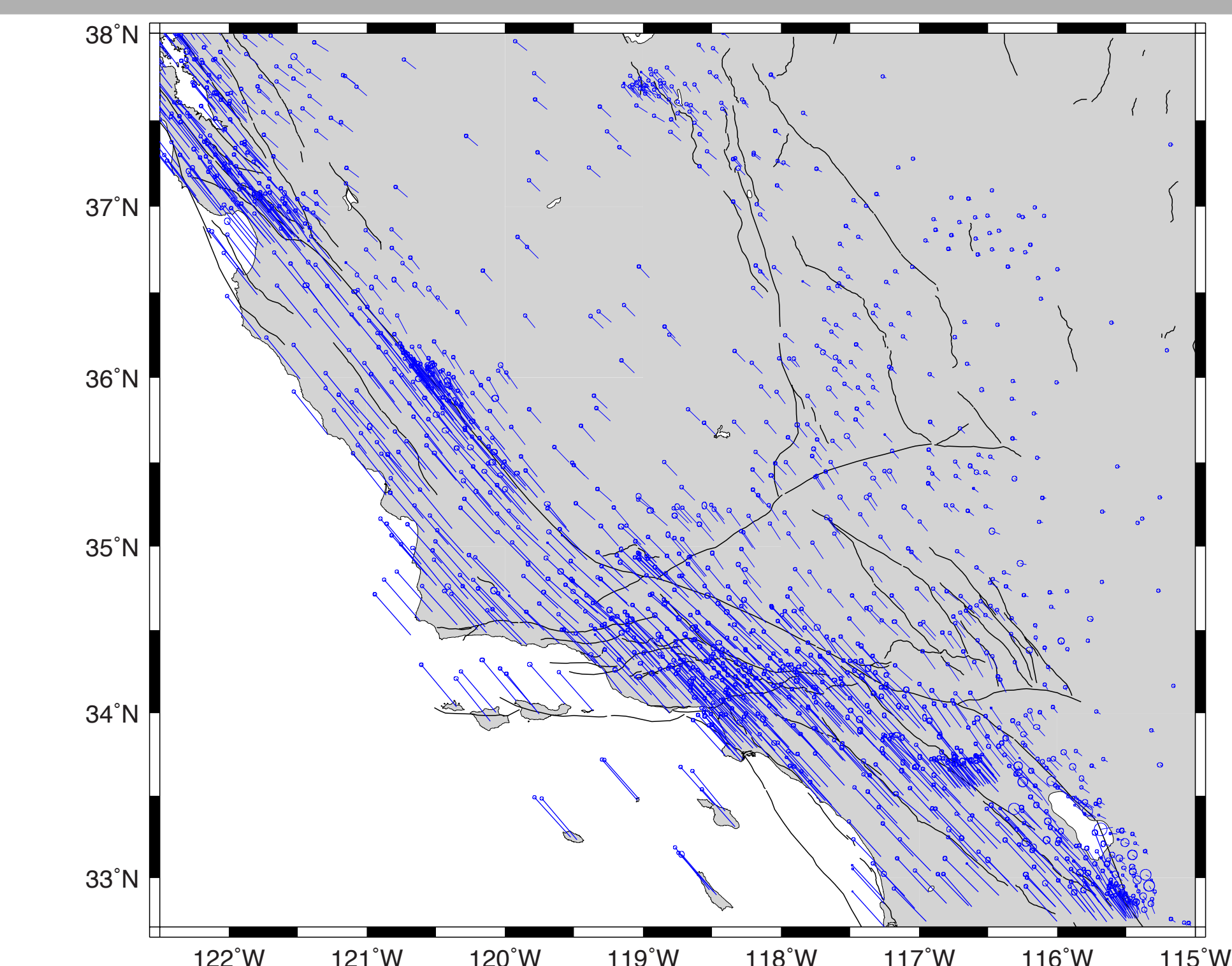
(1) Abstract

The SCEC community is constructing and updating a suite of models for the Southern California region to facilitate cross-disciplinary research (CFM, CVM, CGM, CSM, and CRM). Here we are concerned with the development of the Community Geodetic Model (CGM). Eventually the CGM will consist of vector deformation time series at ~1 km resolution, and better than seasonal sampling. As a first step we are constructing a 0.01° resolution grid of horizontal vector velocities and 2-D tensor strain rate covering the areas of interest to SCEC scientists. Our approach is to first assemble 15 available velocity and strain rate models for the SCEC region. There were 4 main approaches to model construction: isotropic interpolation, interpolation guided by known faults, interpolation of a rheologically-layered lithosphere, and model fitting using deep dislocations in an elastic layer or a half space. We then evaluate the 15 strain rate models in terms of roughness, cross correlation, seismicity rate, and SHmax to select a subset of 10 usable models. Since all the models are based on slightly different geodetic data and use a variety of reference frames, we re-gridded velocities from the 10 models at a 0.01° grid spacing. This is accomplished by forcing each velocity model to match the best available GPS velocity data for the region. The 10 velocity models were averaged and their standard deviation was also computed. Standard deviations are generally small (< 0.5 mm/yr) in areas of good GPS coverage; areas of large standard deviation illustrate where InSAR velocities will contribute most. This uniform velocity is a first step in the development of the full 3-D time dependent CGM. This result is important for seismic hazard evaluation as well as InSAR time series analysis. As new GPS and InSAR data become available this SCEC community model will continue to evolve. The full compilation of the GPS velocity data, the contributed models, and the consensus products will be available on the SCEC web site.

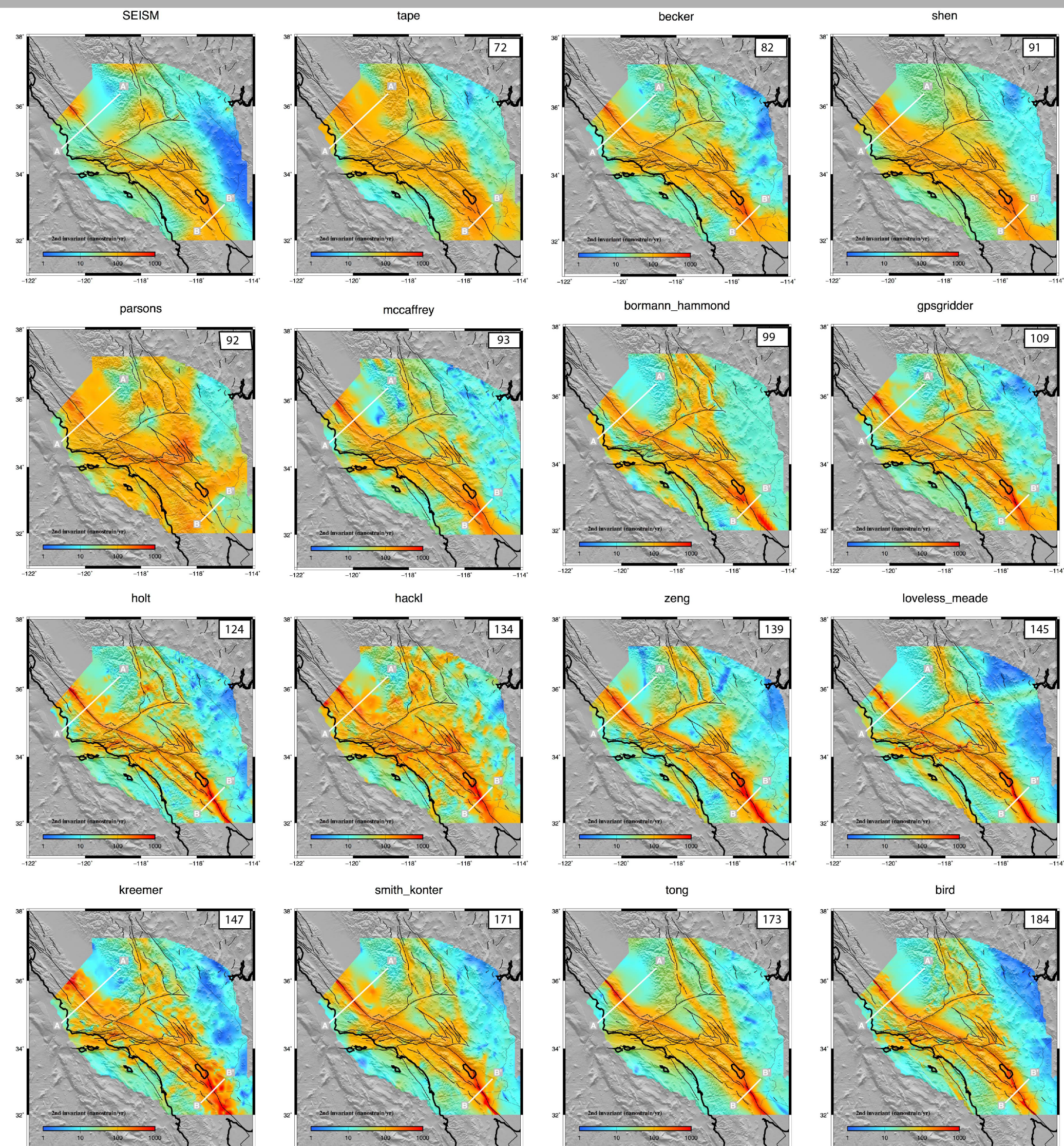
(2) Uses of Horizontal Velocity Grid

Why are we constructing a uniform velocity grid when crustal deformation is a complex time series related to all types of transient processes?

- Velocity and strain rate uncertainties expose areas of weak GPS coverage as well as regions of high temporal variability.
- The uniform velocity model is useful for constraining long-wavelength errors in InSAR analyses.
- Strain rate maps and their uncertainties are useful for off-fault hazard assessment.

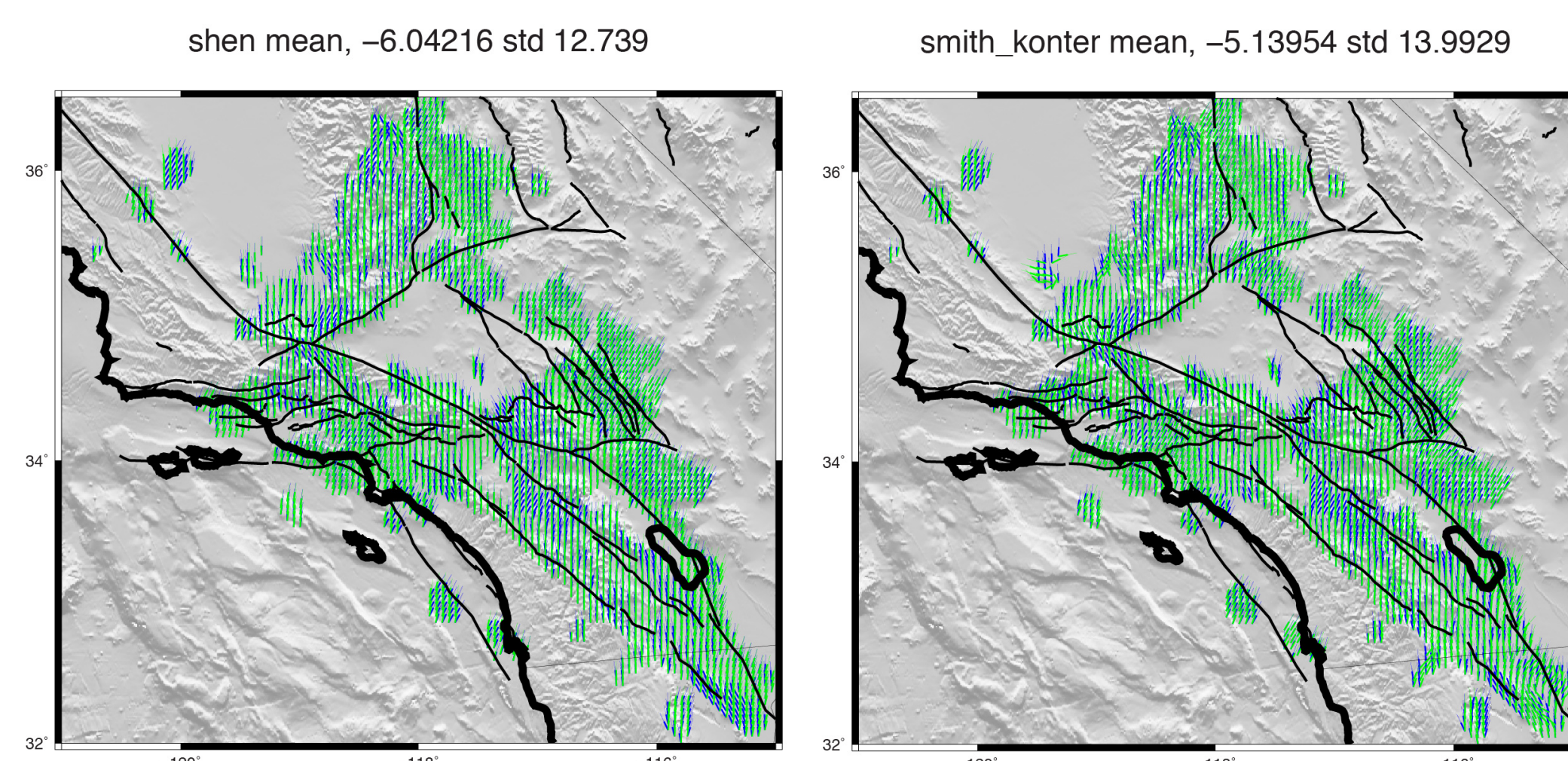


(3) GPS Data GPS velocity vectors (1339) and uncertainties in the Stable North America Reference Frame (SNARF). Contributions from Zeng and Shen [2016b], McCaffrey et al., [2013], and Crowell et al., [2013].



(4) Second Invariant of Strain Rate ordered from smoothest model (tape) to roughest model (bird). The background seismicity rate M 5.0 to 7.0 [Peterson et al., 2008] was scaled into the log of the second invariant to enable cross correlation. Profiles A - A' and B - B' have high density GPS arrays so the actual strain rate can be measured.

(5) Comparisons with SHmax



Comparison between SHmax [blue Yang and Hauksson, 2013] and direction of maximum compression where the second invariant exceeds 10 nanostrain/yr. (left) smooth shen model and (right) rough smith_konter model.

(6) Assessment of the 15 Models

Table 1. Velocity and strain rate models contributed to the CGM

NAME	MODEL VEL	MODEL STRAIN RATE	STRAIN RATE EVAL.			PUBLICATION
			rms	SHmax	corr	
becker	O	X	81	14.5	.76	Platt and Becker, 2010
bird	X	X	183	19.2	.58	Petersen et al., 2014; Field et al., 2014
bornmann_hammond	X	X	99	19.2	.64	Johnson et al., 2013
gpsgridder	X	X	109	17.1	.77	Sandwell and Wessel, 2016
hackl	X	X	134	26.1	.70	Hackl, 2009
holt	X	X	124	18.3	.73	Flesch et al., 2000
kreemer	X	X	152	20.4	.71	Kreemer et al., 2014
loveless_meade	X	X	147	19.1	.64	Loveless and Meade, 2011
mccauffrey	X	X	92	17.6	.60	McCaffrey, 2015
parsons	O	X	92	24.4	.42	Parsons et al., 2006
shen	X	X	91	12.7	.74	Shen et al., 2015
smith_konter	X	X	171	14.0	.63	Smith-Konter and Sandwell, 2009
tape	O	X	73	26.1	.66	Tape et al., 2009
tong	X	X	173	15.4	.60	Tong et al., 2013
zeng	X	X	139	14.0	.72	Zeng and Shen, 2016a

The rms column is the rms of the second invariant of the strain shown in Box (4). The SHmax is the standard deviation in degrees of the difference between the orientation of the direction of maximum compression and SHmax from seismic moment tensors [Yang and Hauksson, 2013]. The corr column is the average of the cross correlation of each model with all the other models in the set. Boxes shaded in grey were not used in the consensus CGM model because of the following reasons. The bornmann_hammond model did not completely cover the region of interest. The becker, parsons, and tape models have no velocity grid. The hackl, parsons, and tape models had very poor fit to SHmax.

(7) Polishing and Averaging of 10 Models

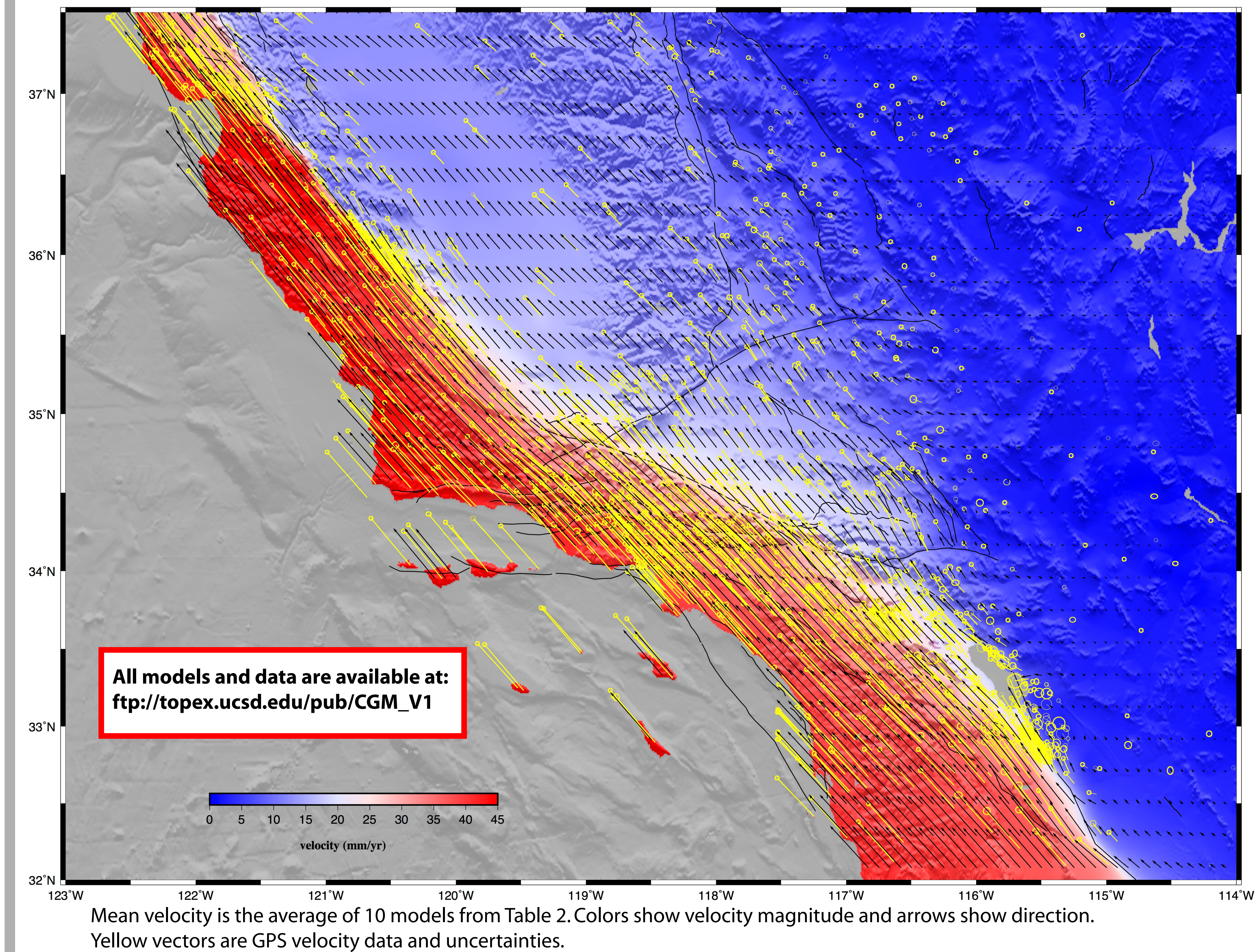
Table 2. Analysis of 10 models used for the CGM

model	GPS mm/yr		MEAN model mm/yr		second invariant nanostrain/yr
	rms	rms masked	rms	rms masked	
mean	0.92	0.85	-	-	119
zeng	1.04	0.94	0.33	0.13	139
gpsgridder	1.03	0.95	0.37	0.16	109
bird	1.02	0.95	0.33	0.16	184
smith_konter	1.04	0.92	0.35	0.17	171
holt	0.99	0.89	0.26	0.16	124
tong	1.07	0.98	0.28	0.18	173
loveless_meade	1.08	0.96	0.28	0.21	145
mccauffrey	0.85	0.74	0.31	0.27	93
shen	0.81	0.74	0.64	0.27	91
kreemer	1.11	0.96	0.44	0.36	147

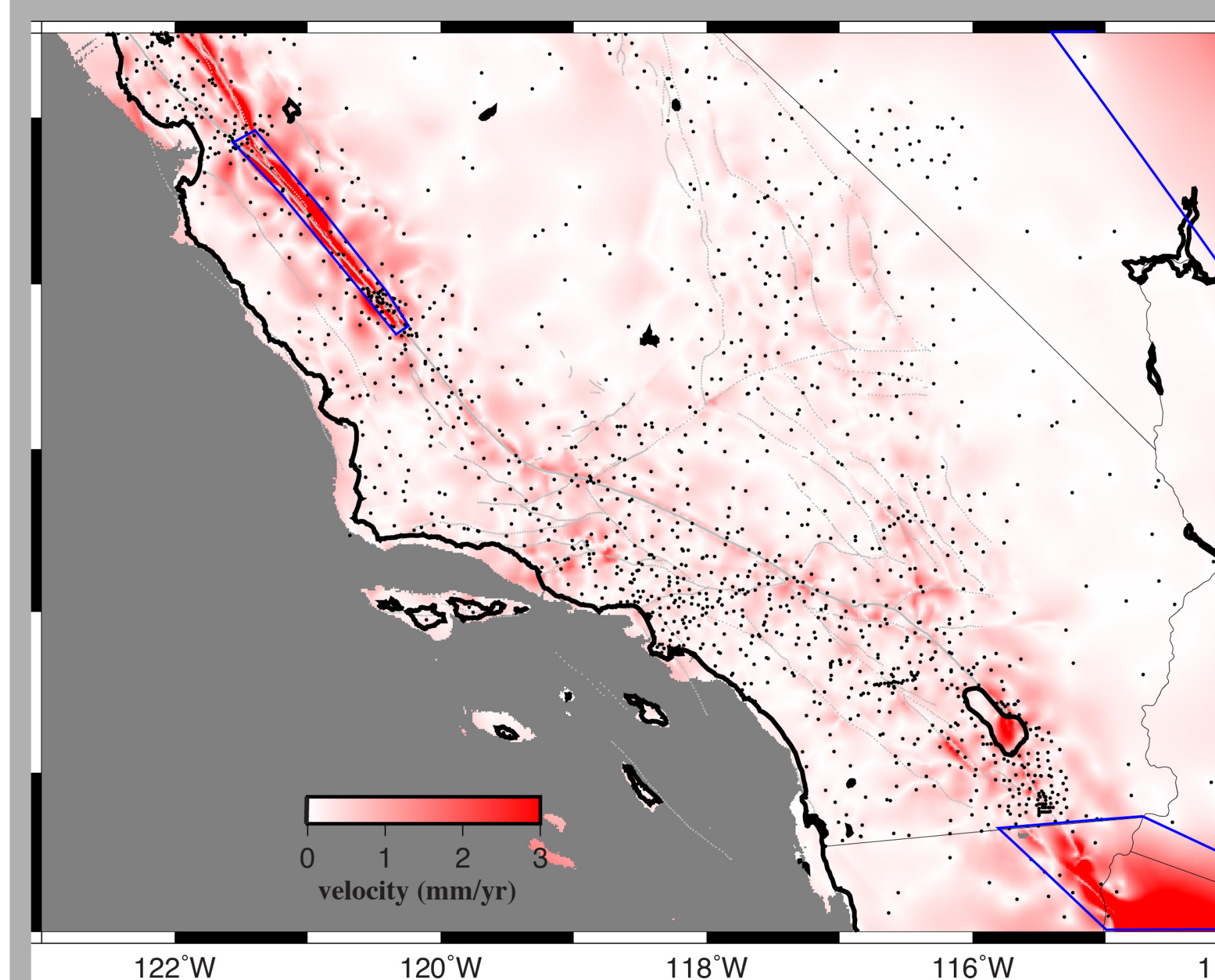
Note that each of the models was adjusted to match the 1339 velocity vectors in the region (see Box 3). This was done using a remove/interpolate/restore method [Sandwell and Wessel, 2016]. The interpolation method does not fit the GPS vectors exactly with the typical rms difference is 1 mm/yr, and slightly smaller when the points in the creeping section are excluded. The rms difference between the mean model and the individual models was also computed with and without the masked areas shown in the velocity standard deviation.

References

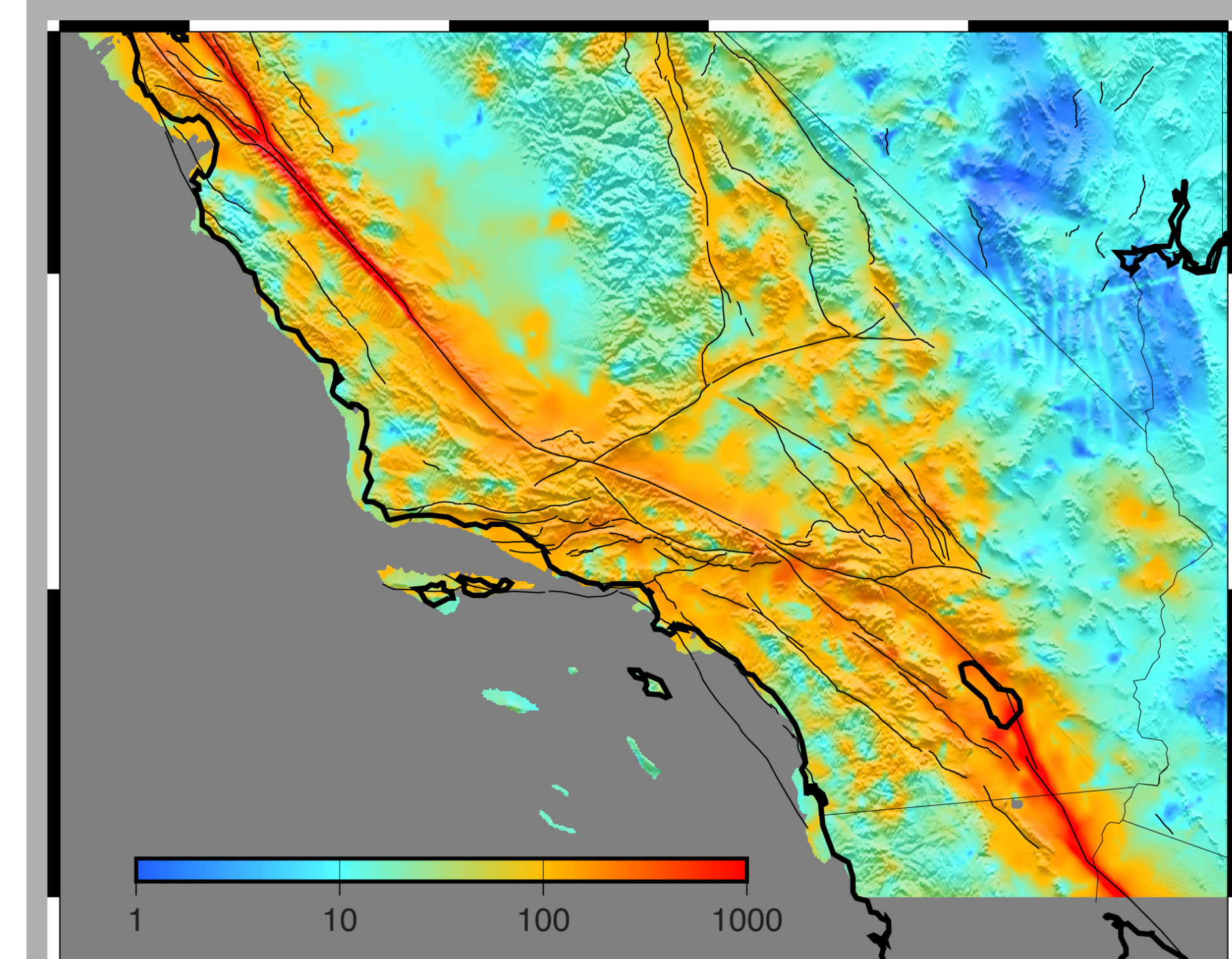
- Bennett, R. W., Rodi, D., and R. Reilinger, Global Positioning System constraints on fault slip rates in southern California and northern Baja, Mexico. *J. Geophys. Res.*, 101, B10, 21943-21960, 1996.
- Bird, P., Long-term fault slip rates, distributed deformation rates, and forecast of seismicity in the western United States from joint fitting of community geologic, geodetic, and stress-direction datasets. *J. Geophys. Res.*, 114, B11403, doi:10.1029/2009JB006317, 2009.
- Crowell, B. W., Y. Bock, D. T. Sandwell, and Y. Falco (2013), Geodetic investigation into the deformation of the Salton Trough. *J. Geophys. Res.*, Solid Earth, 118, doi:10.1002/jgrd.50347.
- Field, E. H., Arrowsmith, R. J., Biasi, G. P., Bird, P., Dawson, T. E., Felzer, K. R., & Zeng, Y. (2014). Uniform California Earthquake Rupture Forecast, Version 3 (UCERF3)—The Time-Independent Model. *Bulletin of the Seismological Society of America*, 104(3), 1122-1180.
- Flesch, L. M., Holt, W. E., Haines, J. J., & Shen, Y. (2000). Dynamics of the Pacific-North American plate boundary in the western United States. *Science*, 287(5454), 834-836.
- Genrich, J. F., Y. Bock, and R. G. Mason, Crustal deformation across the Imperial Fault: Results from kinematic GPS surveys and trilateration of a densely-spaced, small-aperture network. *J. Geophys. Res.*, 102, 4985-5004, 1997.
- Gonzalez-Ortega, J. A., Y. Falco, D. Sandwell, F. A. Nava Pichardo, J. Fletcher Mackrinn, J. J. Gonzalez Garcia, B. Lipovsky, M. Floyd y G. Funning, El Mayor-Cuicapi (Mw 7.2) earthquake: Early near-field postseismic deformation from InSAR and GPS observations. *Journal of Geophysical Research*, Solid Earth, 119(2), 1462-1497, 2014.
- Hackl, M., R. Malservais, and S. Wdowinski, Strain pattern from dense GPS networks. *Nat. Hazards Earth Syst. S.*, 1177-1187, 2009.
- Hearn, E., K. Johnson, D. Sandwell, and W. Thatcher, SCEC UCERF workshop report: http://www.scec.org/workshops/2010/gps-uc3/FinalReport_GPS-UCERF3Workshop.pdf, 2010.
- Johnson, K., P. Bird, Y. Zeng, W. Thatcher, T. Dawson, R. Weldon, R. McCaffrey, W. C. Hammond, J. Bornmann, T. Herring, 2013. Geodetically derived deformation models for UCERF3, report for the Working Group on California Earthquake Probabilities, available at <http://wgceep.org>.
- Kreemer, C., G. Blewitt, and E. C. Klein (2014), A geodetic plate motion and Global Strain Rate Model. *Geochim. Geophys. Geost.*, 15, 3849-3889, doi:10.1002/2014GC005407.
- Lindsay, E. O., Falco, Y., Bock, Y., Sandwell, D. T., & Bilham, R. (2014). Localized and distributed creep along the southern San Andreas Fault. *Journal of Geophysical Research: Solid Earth*, 119(10), 7909-7922.
- Loveless, J. P., & Meade, B. J. (2011). Stress modulation on the San Andreas fault by interseismic fault system interactions. *Geology*, 39(11), 1035-1038.
- Lyons, S. N., Y. Bock, and D. T. Sandwell, Creep along the Imperial Fault, southern California, from GPS measurements. *J. Geophys. Res.*, 107(B10), 2249, doi:10.1029/2001JB000763, 2002.
- McCaffrey, R., King, R. W., Payne, S. J., & Lancaster, M. (2013). Active tectonics of northwestern US inferred from GPS-derived surface velocities. *Journal of Geophysical Research: Solid Earth*, 118(2), 709-723.
- McCaffrey, R. (2015). Time-dependent deformation of California from inversion of GPS time series. SCEC annual meeting.
- Parsons, T., Tectonic stressing in California modeled from GPS observations. *J. Geophys. Res.*, 111, doi:10.1029/2005JB003946, 2006.
- Parsons, T., K. M. Johnson, P. Bird, J. M. Bornmann, T. E. Dawson, E. H. Field, W. C. Hammond, T. A. Herring, R. McCaffrey, Z. K. Shen, W. R. Thatcher, R. J. Weldon and Y. Zeng, 2013. Appendix C: Deformation models for UCERF3. USGS Open-File Report, v. 2013-1165, 66 pp. http://pubs.usgs.gov/of/2013/1165/pdf/of2013-1165_appendixC.pdf.
- Petersen, M. D., Mueller, C. S., Frankel, A. D., & Zeng, Y. Appendix J: Spatial Seismicity Rates and Maximum Magnitudes for Background Earthquakes, USGS Open File Report 2007-1437J, 2008.
- Shen, Z.-K., R. King, D. C. Agnew, M. Wang, T. A. Herring, D. Dong, and P. Fang (2011). A unified analysis of crustal motion in southern California, 1970-2004: The SCEC crustal motion map. *Journal of Geophysical Research*, v. 116, B11402, doi:10.1029/2011JB008549.
- Shen, Z.-K., Wang, M., Zeng, Y., & Wang, F. (2015). Optimal interpolation of spatially discretized geodetic data. *Bulletin of the Seismological Society of America*, 105, 2117-2127.
- Smith-Konter, B., D. T. Sandwell, Stress evolution of the San Andreas Fault System: recurrence interval versus locking depth. *Geophys. Res. Lett.*, 35, L13304, doi:10.1029/2009GL012735, 2009.
- Tape, C., P. Mose, M. Simons, D. Dong, and F. Webb, Multiscale estimation of GPS velocity fields. *Geophys. J. Int.*, 179, 945-971, 2009.
- Tong, X., D. T. Sandwell, and B. Smith-Konter (2013). High-resolution interseismic velocity data along the San Andreas Fault from GPS and InSAR. *J. Geophys. Res.*, Solid Earth, 118, doi:10.1029/2012JB008442.
- Yang, W., and E. Hauksson (2013). The tectonic crustal stress field and style of faulting along the Pacific North America Plate boundary in southern California. *Geophys. J. Int.*, 194, doi:10.1093/gjg/ggt113.
- Zeng, Y. and Z.-K. Shen (2016a). A Fault-Based Model for Crustal Deformation, Fault Slip Rates and Off-Fault Strain Rate in California. *BSSA*, 106(2), doi:10.1785/0120140250.
- Zeng, Y. and Z.-K. Shen (2016b). A Fault-Based Model for Crustal Deformation in the Western United States Based on a Combined Inversion of GPS and Geologic Inputs. *BSSA*, in press.



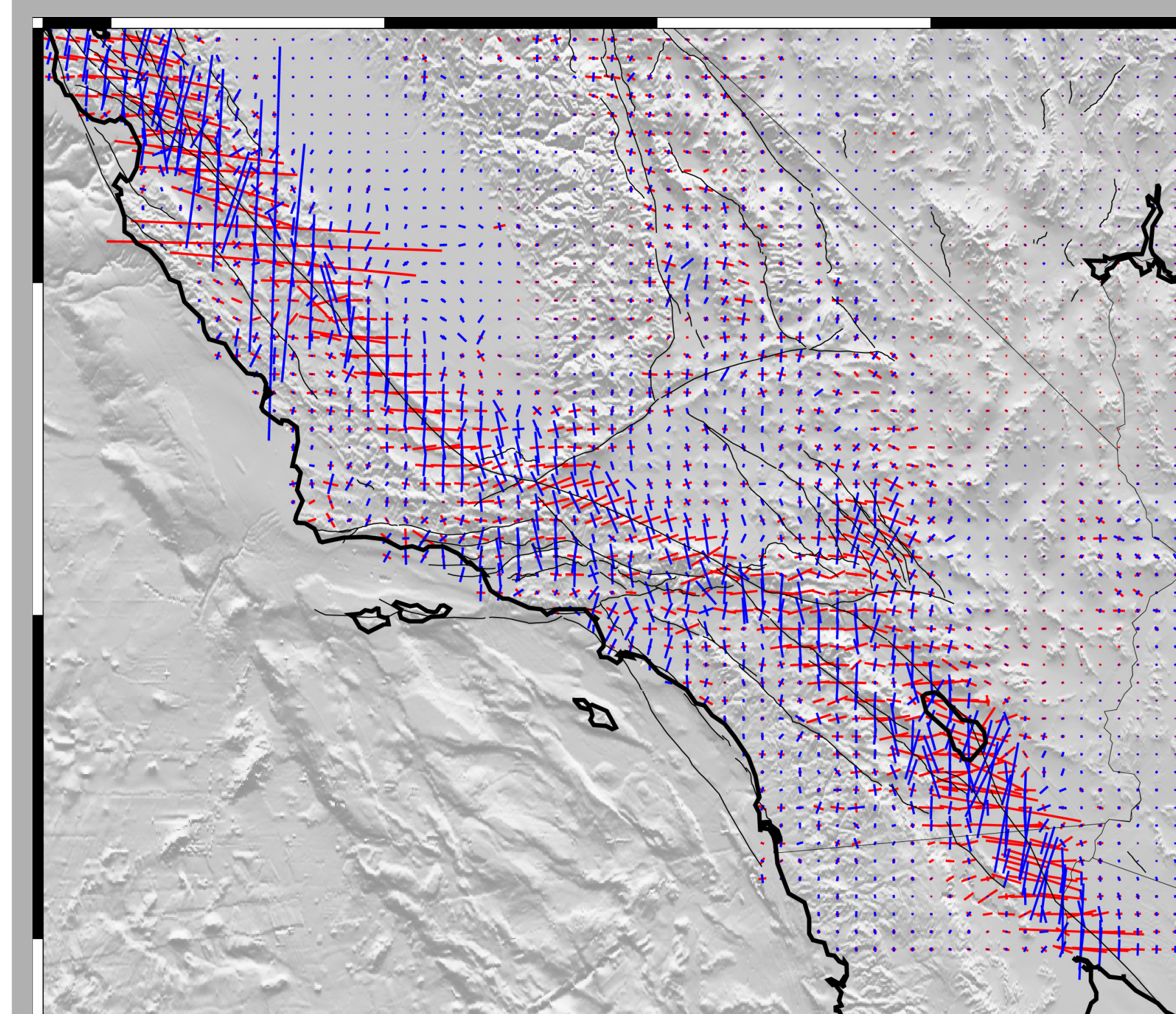
Mean velocity is the average of 10 models from Table 2. Colors show velocity magnitude and arrows show direction. Yellow vectors are GPS velocity data and uncertainties.



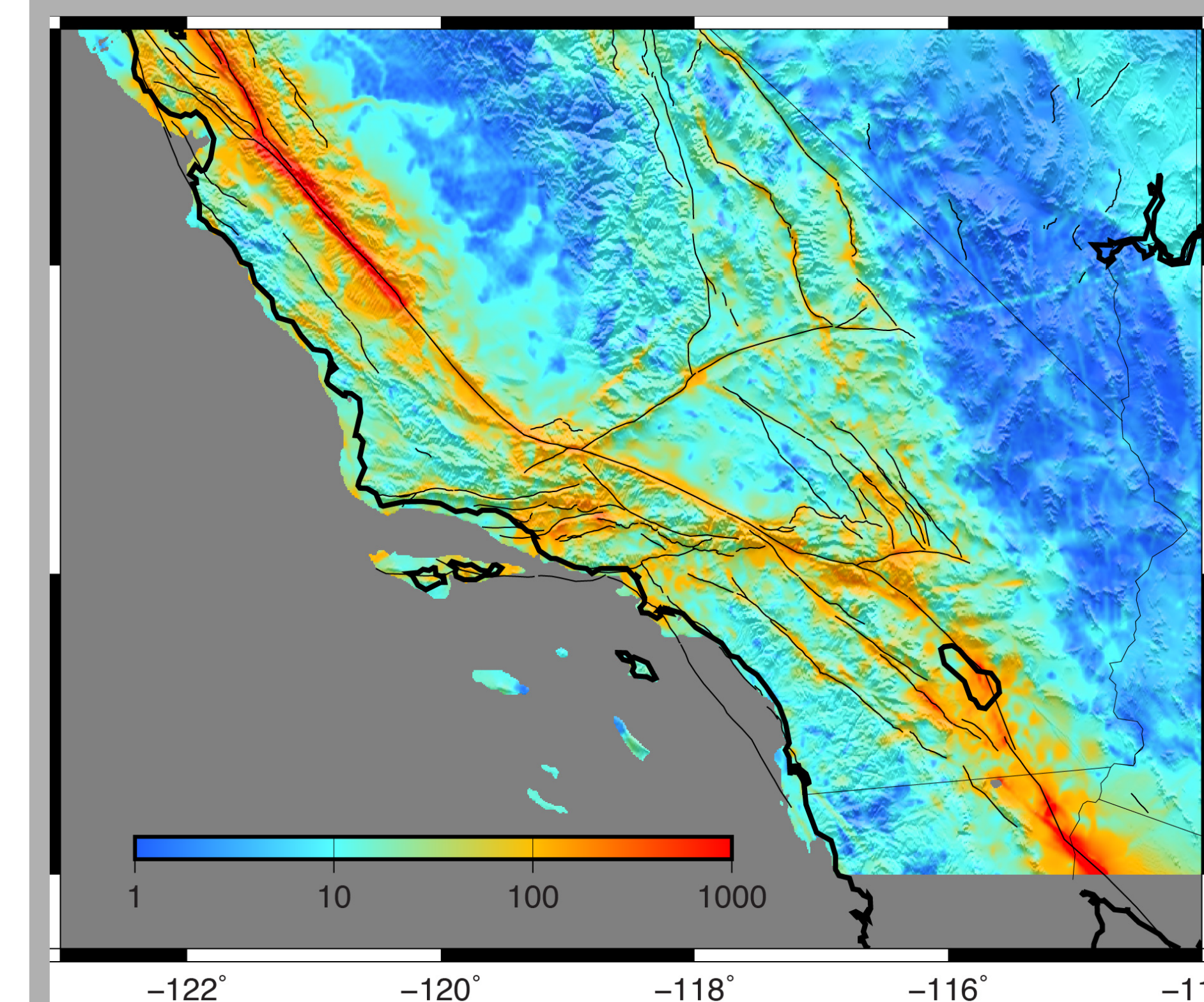
Standard deviation of vector velocity from mean velocity. Blue outlines regions where the GPS data cannot resolve the velocity to better than ~1 mm/yr.



Average second invariant of strain rate from 10 models.



Average strain rate tensor from 10 models.



Standard deviation of second invariant of strain rate with respect to the mean of from 10 models.